CHAPTER - 6

AN IMPROVED INVERSION ALGORITHM FOR SPATIO-TEMPORAL RETRIEVAL OF SOIL MOISTURE THROUGH MODIFIED WATER CLOUD MODEL USING C- BAND SENTINEL -1A SAR DATA

6.1 INTRODUCTION

Surface soil moisture plays an important role for describing water and energy exchanges at the land surface. The continuous observations of soil moisture (SM) are essential for the crop yield prediction, hydrology, ecology, agriculture and meteorology (Petropoulos et al. 2018; Torres-Rua et al. 2016). Therefore, the retrieval of soil moisture and surface roughness using microwave remote sensing plays a vital role for water-management processes, agricultural applications, and monitoring of floods, droughts and ecosystem etc.

The microwave has specific properties like both day/night data acquisition capability, acquisition in all weather conditions and high penetrating power etc. It has various applications in the areas of remote sensing, plasma physics and communication technology (Mishra et al. 2017; Malik 2014; Malik and Aria 2013; Lievens and Verhoest 2011; Malik and Aria 2010; Malik 2008; Aria and Malik 2009; Malik 2004).

In the past decade, Synthetic Aperture Radar (SAR) remote sensing techniques have demonstrated its high potential to retrieve SM over different type of soil field covers (Kumar et al. 2018; Aubert et al. 2013; Morvan et al. 2008). However, retrieving SM under different vegetation condition (sparse and dense vegetation) using microwave remote sensing is a tedious task because of vegetation covered volume scattering, underlying soil surface scattering and its own moisture content (Bindlish and Barros 2001, Bruckler et al. 1988). The

radar signal follows a nonlinear behavior with the soil surface parameters. Therefore, soil parameters show strong relationship with radar backscattering at the L - band (0.5 – 1.5 GHz), C - band (4 – 8 GHz) whereas lowest relationship is observed at X - band (8 – 12 GHz) (Du et al. 2015; Oh et al. 1992). However, its sensitivity is high at higher incidence angles at all L -, C - and X - bands (Liu 2016; Hosseini et al. 2015; Baghdadi et al. 2012; Zribi and Dechambre 2002).

Various empirical, physical and regression models have been employed to retrieve SM using SAR and optical satellite data from the different platforms. In the recent past, several researchers have studied, both passive and active sensors, for assessing the sensitivity of microwave emission and backscattering to soil moisture in different environmental conditions and various vegetation covers (Notarnicola et al. 2006; Ulaby et al.1984; Santamaria et al. 2016). Kumar et al. (2015) proposed the soil moisture estimation using water cloud model (WCM) using different vegetation descriptors. They concluded that LAI can be treated as the best vegetation descriptor for the retrieval of the SM. Bao et al. (2018) developed the Modified WCM with built of spectral index parameters in original WCM for the estimation of surface SM over vegetated area by synergy of Sentinel -1A and Landsat-8 satellite data. Kumar et al. (2018) used various regression models (random forest, support vector machine and artificial neural network) for the estimation of soil moisture covered by different crops and their soil variability. They found the SM retrieval more accurate at VV polarization than VH polarization using three different models.

The WCM is often used for retrieving SM and modeling of the scattering of vegetated areas because of its less complexity for inversion techniques and using minimum number of input parameters. Several vegetation descriptors such as plant height (PH), leaf water area index (LWAI), leaf area index (LAI), vegetation water content (VWC), and normalized difference vegetation index (NDVI) have been used in WCM. LAI plays as a good vegetation

descriptor parameter in WCM for more accurate retrieval of SM. The WCM was subsequently modified or extended by various authors for accurate retrieval of SM in vegetated regions. Li and Wang (2018) introduced SAR derived vegetation descriptors in WCM for the retrieval of SM using dual-polarized Radarsat - 2 satellite data. Furthermore, Gao et al. (2017) proposed synergetic use of Sentinel - 1A SAR and Sentinel - 2 optical data for the operational use of high resolution mapping of SM over agricultural regions. Baghdadi et al. (2017) prepared new approach in WCM for the estimation of SM over vegetated areas with combined use of the Sentinel - 1 SAR data with Sentinel - 2 optical data.

The iterative optimization (IO) algorithms have difficulty in finding the global minima for nonlinear problems while look up table (LUT) technique have a lower generalization capability. These factors reduce the efficiency of inversion results. Alternatively, the researcher have opted the machine-learning regression algorithms to fix these kinds of model errors and enhance the capability of WCM parameterization. Among various machine - learning algorithms (ANN, SVM and linear regression), the RFR (random forest regression) showed more robustness due to its less impact on outliers and needs fewer model parameters setting. Kumar et al (2018) performed the study for the estimation of LAI using ANNR, SVR RFR and LR machine–learning algorithm and demonstrated high correlation and low root mean square error (RMSE) for RFR algorithm in comparison to other regression techniques for the estimation of LAI.

In the present study, the main focus is to investigate the capability of the C-band Sentinel - 1A SAR data to retrieve spatio-temporal SM in sparse vegetated (region - 1) and vegetated (region - 2) soil fields through MWCM. The modification of MWCM was done by introducing a vegetation fraction (f_{veg}) parameter, computed from Landsat - 8 satellite data, in WCM model. For this purpose, satellite images were acquired at three acquisition dates in good weather and in less contaminated conditions. The computational algorithms for the

retrieval of SM using MWCM adopted following major steps: (1) the non-linear least square optimization techniques were used for parameterization of MWCM using training data sets; (2) furthermore, the look-up table (LUT) algorithm was used to build the random forest (RF) regression model; (3) the Multi-target random forest regression (MTRFR) algorithm was adopted with a regularization routine for a stable and optimum solution related to the inversion of the MWCM. Therefore, the validation of the developed model was done by using independent data sets like simulated backscattering coefficient and LAI as predictors and the SM as the response for the retrieval of spatio-temporal variation of SM in the proposed study areas.

6.2 STUDY AREA AND DATA COLLECTION

6.2.1 Study area

A part of Varanasi district in India was chosen for the retrieval of SM using proposed methodology. The study area lies at an average height of 81 m above the mean sea level and center latitude 25° 17′ 51″ N and longitude 82° 56′ 36″ E covering a total area of 192 km^2. It is one of the holy cities in India located near the holy river Ganges. A moist subtropical climate with seasonal variations between winter and summer temperatures is found in Varanasi district. In this region, the soil texture changes greatly across the sampling site which results in large variation of SM. It has very fertile and wealthy natural conditions for agriculture purposes because of its location in Indo-Gangetic plane, as shown in Figure 6.1.

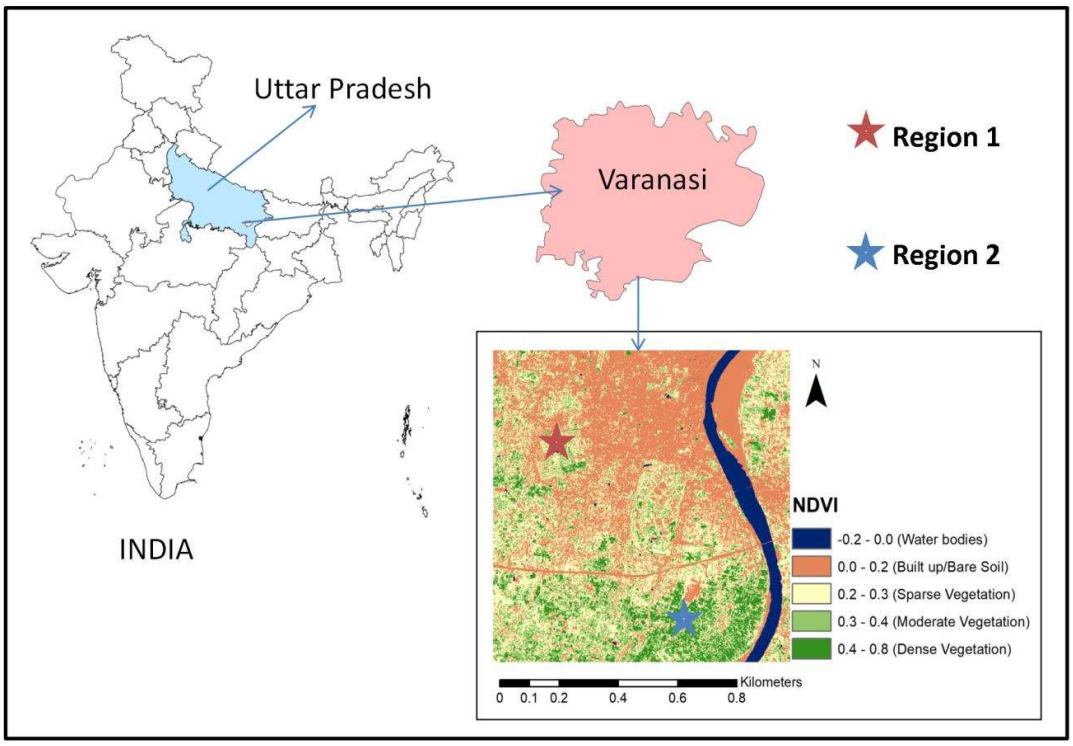

Figure 6.1. Location map of the study area

6.2.2 Satellite data collection and processing

The Sentinel-1A and Landsat-8 satellite images were acquired on 19/12/2016, 05/02/2017 and 25/03/2017 for the present study. The central frequency of the SAR sensor is 5.405 GHz (C - band). The primary image preprocessing of SAR data was completed using SNAP tools with geometric correction and radiometric calibration. An enhanced Lee filter was carried out to reduce the speckle noise. SAR intensity image was converted into dB from the linear scale (Filipponi, 2019). The Landsat-8 optical images were used for this study to compute f_{veg} as a vegetation fraction parameter in MWCM. The radiometric calibration and atmospheric correction were performed using ENVI - 5.1 (Bala et al. 2019). At last, the images were co - registered according to Sentinel - 1A. The full details of satellite data is summarized in Table 6.1.

Table 6.1. Satellite data specifications

A) SAR (Synthetic Aperture Radar) data.						
Satellite	Date of Acquisition	Mode	Polarization	Product type	Resolution (m × m)	Level
Sentinel-1A	19/12/2016	IW	VV/VH	GRD	5 × 20	L 1
	05/02/2017	IW	VV/VH	GRD	5 × 20	L 1
	25/03/2017	IW	VV/VH	GRD	5 × 20	L 1
B) Optical data						
Satellite	Date of Acquisition	No. of bands	Spatial resolution (m)	Radiometric resolution	Swath (km)	Level
Landsat -8 (OLI)	19/12/2016	11	30	12-bit	185	L 1
	05/02/2017	11	30	12-bit	185	L 1
	25/03/2017	11	30	12-bit	185	L 1

6.2.3. In-situ measurements

6.2.3.1 Soil moisture (SM)

The surface SM is influenced by physical and chemical properties of Earth surfaces such as dielectric and soil roughness etc. The soil sampling was performed simultaneously with the dates of acquisition of satellites images (19/12/2016, 05/02/2017 and 25/03/2017).The soil samples collected from the three type of soil fields were dried in an oven at 110 °C for 18 - 20 hrs. (Younis and Iqbal 2015; Gardner. 1986). These different types of samples were weighted before and after dryness for computing surface SM. The average values of the soil moisture content were taken to compute the percent of SM. The soil moisture can be obtained using the relation given as:

$$\mathrm{SM}(\%) = \frac{W_{wet} - W_{dry}}{W_{dry}} \times 100 \quad (6.1)$$

Where W_{wet} and W_{dry} are the weights of soil samples collected before and after dryness during field observation, respectively.

6.2.3.2 Leaf area index (LAI)

LAI is one of the key growth parameter of crops which characterizes the plant canopies. It is defined as the one-sided green leaf area per unit ground surface area (LAI = leaf area / ground area, m^2 / m^2). The LAI measurements were made in sampling areas using an instrument namely LAI - 2200C plant canopy analyzer (LI - COR, Inc.).The detailed specification of in-situ measurements are summarized in Table 6.2.

Table 6.2 The detailed information of in-situ measurements

Region-1					
Sampling date	Type of soil field	Type of Crops	LAI (m^2/m^2) (min-max)	SM (%) (min-max)	Sapling point
19/12/2016	Sparse vegetated	Lentil, linseed, pea	0.56 – 1.14	3.51 – 21.2	33
05/02/2017	Sparse vegetated		1.31 – 2.34	4.01 – 26.4	33
25/03/2017	Sparse vegetated		1.92 – 3.32	5.41 – 25.6	35
Region-2					
19/12/2016	Vegetated	Wheat, barley	0.98 – 2.10	4.78 – 31.2	31
05/02/2017	Vegetated		2.45 – 3.82	7.67 – 37.4	34
25/03/2017	Vegetated		3.10 – 5.72	8.23 – 39.7	35

6.2.4 Assessment of in-situ measurements with SAR backscattering coefficient ($\sigma^0(\mathrm{dB})$)

The temporal variation with correlation matrix of the measured LAI, SM and computed $\sigma^0(dB)$ using satellite data of the sampling fields for both the regions 1 and 2 are shown in Figures 6.2 and 6.3, respectively. In region 1, the sampling fields were mostly covered by sparse vegetation like lentil, linseed and pea during satellite acquisition period. Figure 6.2 indicates the temporal (19/12/2016, 05/02/2017 and 25/03/2017) changes of the measured values and their correlations in region 1. The Figure 6.3 shows the temporal variation of in-situ measurements and their correlations in region 2 where wheat and barley were dominating crops. The computed $\sigma^0(dB)$ was found highly correlated with the LAI in region 2 (R^2 = 0.76) than the region 1 (R^2 = 0.64). While the SM showed lower correlation with the computed $\sigma^0(dB)$ in both the regions. It is evident that the C - band SAR data is more sensitive to the vegetation canopy and comparatively less sensitive over bare soil covered fields (Inoue et al. 2002).

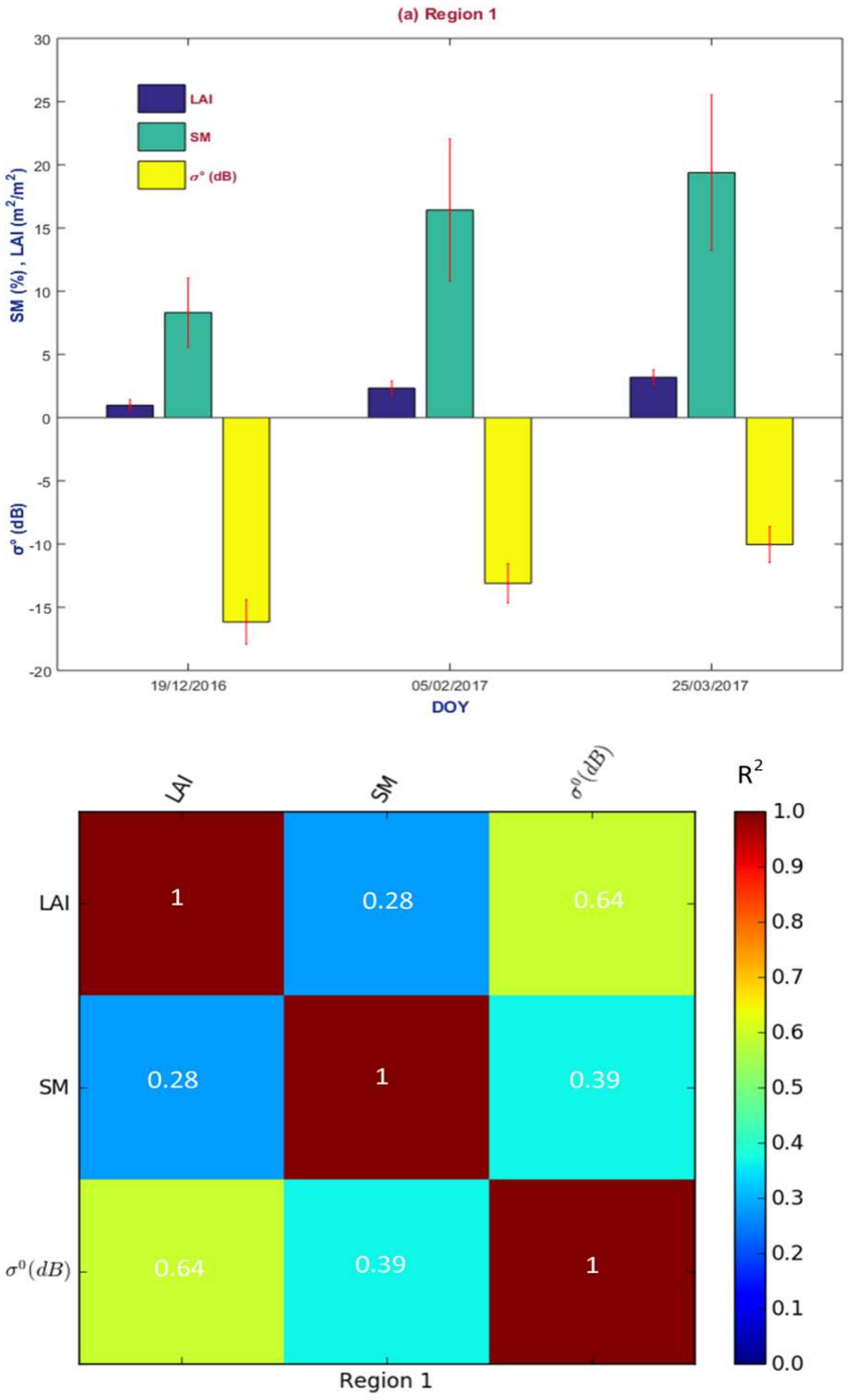

Figure 6.2 The temporal variation of SM, LAI and σ^0 (dB) in region 1 with correlation matrix

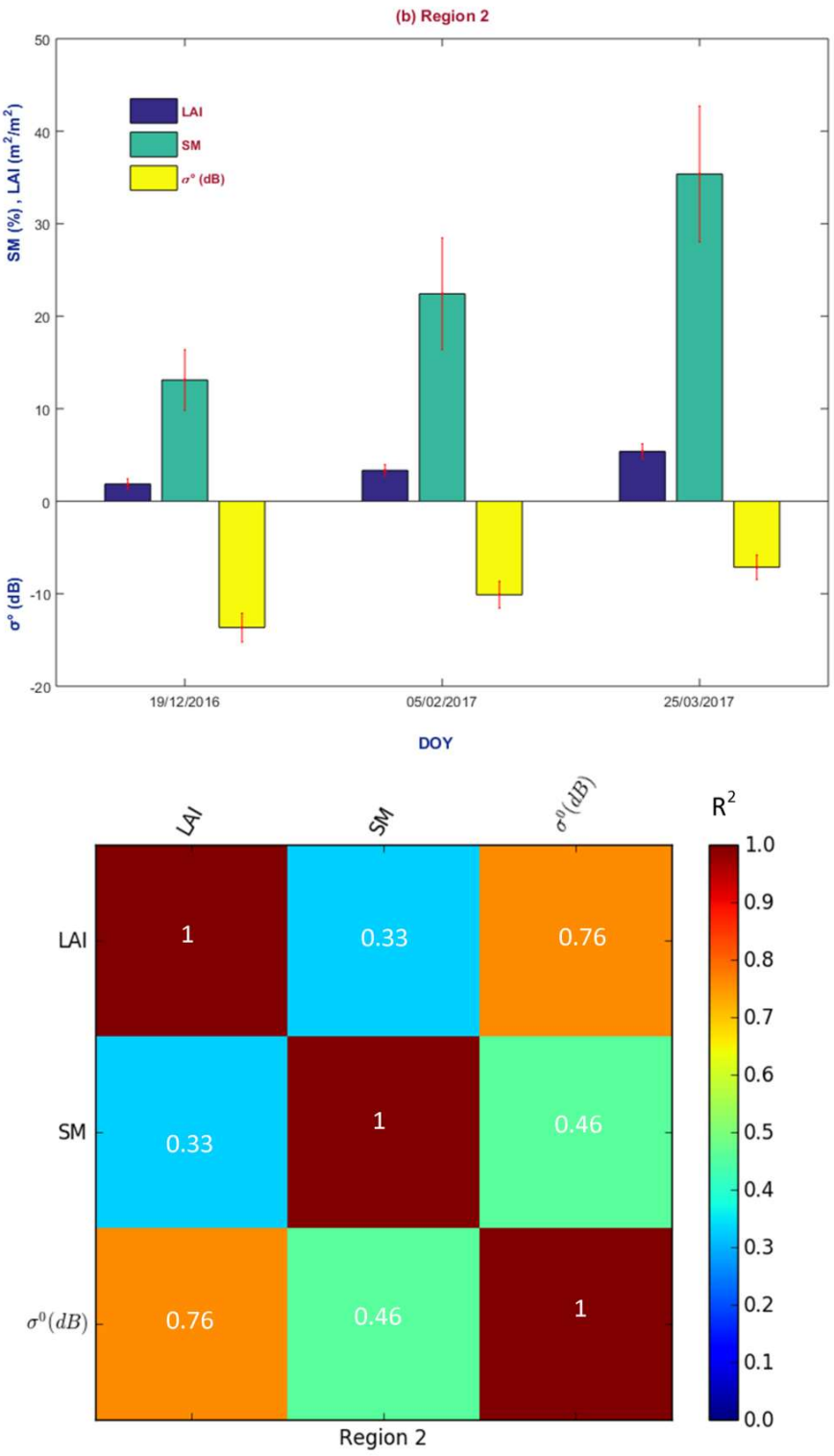

Figure 6.3 The temporal variation of SM, LAI and σ^0 (dB) in region 2 with correlation matrix

6.3. METHODOLOGY

In the present study, a MWCM semi-empirical model was used for the retrieval of spatio-temporal variation of SM in the vegetated soil fields. The illustration of computational approach for the SM retrieval is shown in Figure 6.4.

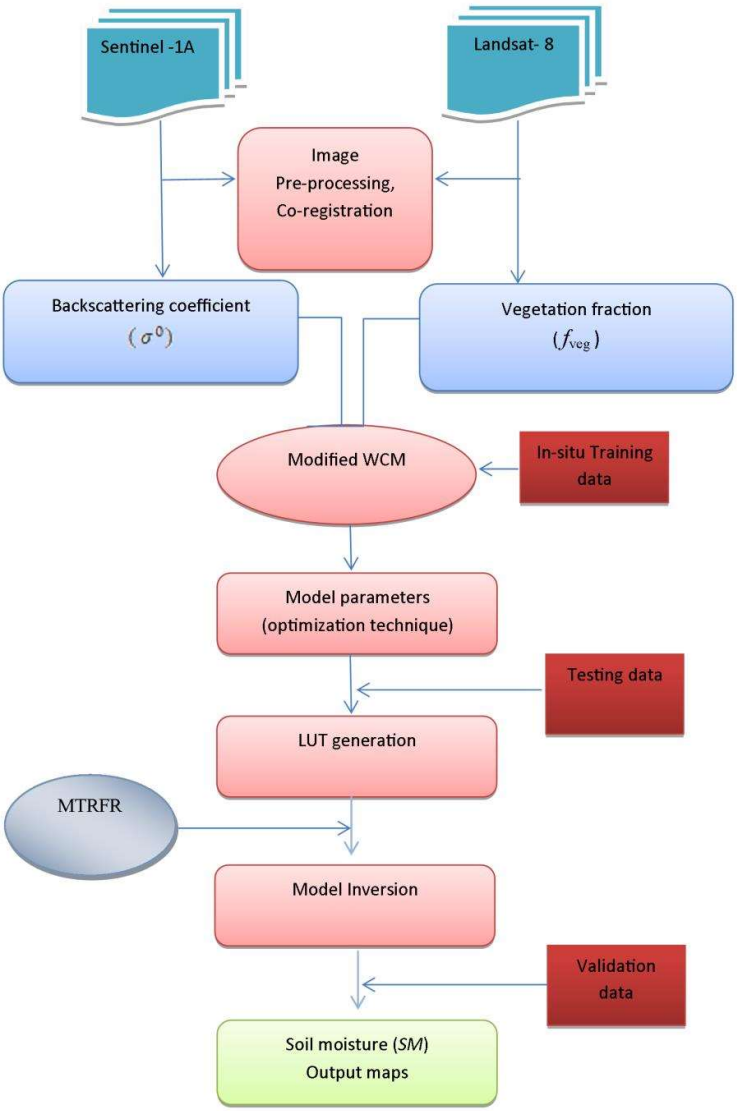

Figure 6.4. Methodology flow chart for the retrieval of SM using MWCM

6.3.1. Modified water cloud model (MWCM)

In WCM, the vegetation canopy and vegetation layer were assumed as a homogeneous anisotropic scatterer in order to ignore the multiple scattering effects between vegetation and soil (Ulaby et al. 1982a; Prasad 2011; Kumar et al. 2012). The total backscatter coefficient was mainly composed of volume scattering generated from the direct backscattering of the vegetation and the soil surface after the double attenuation, as follows

$$\sigma^0(dB) = \sigma^0_{veg} + \tau^2\sigma^0_{soil} \tag{6.2}$$

Where σ^0_{veg} represents the backscattered radar signal from vegetation canopy and σ^0_{soil} is the backscattering response from the soil surfaces. Whereas τ^2 is defined as the two-way attenuation factor through vegetation-soil interfaces.

$$\sigma^0(dB) = f_{veg}AV^E cos\theta\left[1 - e^{-\left(\frac{2BV}{COS\theta}\right)}\right] + \left\{\left(1 - f_{veg}\right)[C + D(\mathrm{SM})]e^{-\left(\frac{2BV}{COS\theta}\right)}\right\} \tag{6.3}$$

Therefore, the general expression of SM obtained by numerical inversion of Equation (6.3) can be expressed as:

$$SM = \frac{1}{D}\left\{\frac{\sigma^0(dB) - f_{veg}AV^E cos\theta\left[1 - e^{-\left(\frac{2BV}{COS\theta}\right)}\right]}{\left(1 - f_{veg}\right)e^{-\left(\frac{2BV}{COS\theta}\right)}} - C\right\} \tag{6.4}$$

where A, E, B, C and D are model parameters. V_1 is the vegetation descriptor (i.e. LAI), SM is soil moisture and θ is the incidence angle. The f_{veg} is expressed as,

$$f_{veg} = \frac{NDVI - NDVI_{min}}{NDVI_{max} - NDVI_{min}} \tag{6.5}$$

where f_{veg} and NDVI are the vegetation fraction and the normalized differential vegetation index, respectively. The NDVI values of crops were found to be changed with the crop phenology and varying according to their growth period. The $NDVI_{max}$ is the maximum

NDVI value of crops observed in the entire growth stages whereas $NDVI_{min}$ is possible minimum value of NDVI for the bare soil field (Gutman and Ignatov 1998).

6.3.2. Model inversion

In this study, an improved inversion algorithm was used to generated LUT and feed in the MTRFR to tackle the inversion problem. The MWCM inversion includes three significant steps: (a) LUT generation (b) MTRFR algorithm development by utilizing the LUT generated by forward and inverse modeling and (c) spatio - temporal retrieval and mapping of SM in both the regions.

6.3.2.1. Model creation and calibration of MWCM

Model inversion technique was established to retrieve the SM using sentinel -1 A data and in-situ data. The total numbers of pooled datasets corresponding to three different temporal variability of crop growth condition were split into model parameterization (training) and testing datasets (70 % and 30 % of the pooled data, respectively). Besides that, the validation of the MWCM was done by using an independent dataset of crops which was not used in the parameterization of the MWCM. The model parameters namely A, E, B, C and D were determined by the minimization of cost function between the observed and modelled backscattering coefficient using nonlinear least square optimization algorithm (Prasad 2011).

$$cost\ function\ \{\ g(SM)\} = \ \ Minimize\ \left\| \sum_{i=1}^{n} \left(\sigma^0_{ob_i} - \sigma^0_{mod_i}\right)^2 \right\| \tag{6.6}$$

Where σ^0_{ob} and σ^0_{mod} are the computed backscattering coefficients derived from the Sentinel-1A and modelled backscattering coefficients derived by the MWCM, respectively using Equation 6.2 at VV polarization.

For optimality condition of MWCM model, the following constraints were used for computation of model parameters, which can be expressed as:

$$\nabla g = 2D\left(\sum_{\mathrm{i}=1}^{\mathrm{n}}(\sigma_{ob_i}^0 - \sigma_{mod_i}^0)^2\right)^T\left(\sum_{\mathrm{i}=1}^{\mathrm{n}}(\sigma_{ob_i}^0 - \sigma_{mod_i}^0)^2\right) = 0 \qquad (6.7)$$

Therefore, the Derivative matrix (Jacobian) of differentiable function $(\sigma_{ob_i}^0 - \sigma_{mod_i}^0)^2$ can be defined as

$$D\left(\sum_{\mathrm{i}=1}^{\mathrm{n}}(\sigma_{ob_i}^0 - \sigma_{mod_i}^0)^2\right)^T$$

$$= \begin{bmatrix} \frac{\partial(\sigma_{ob_1}^0 - \sigma_{mod_1}^0)^2}{\partial x_1} & \frac{\partial(\sigma_{ob_1}^0 - \sigma_{mod_1}^0)^2}{\partial x_2} & \cdots & \frac{\partial(\sigma_{ob_1}^0 - \sigma_{mod_1}^0)^2}{\partial x_n} \\ \frac{\partial(\sigma_{ob_2}^0 - \sigma_{mod_2}^0)^2}{\partial x_1} & \frac{\partial(\sigma_{ob_2}^0 - \sigma_{mod_2}^0)^2}{\partial x_1} & \cdots & \frac{\partial(\sigma_{ob_2}^0 - \sigma_{mod_2}^0)^2}{\partial x_n} \\ \vdots & \vdots & & \\ \frac{\partial(\sigma_{ob_n}^0 - \sigma_{mod_n}^0)^2}{\partial x_1} & \frac{\partial(\sigma_{ob_n}^0 - \sigma_{mod_n}^0)^2}{\partial x_2} & \cdots & \frac{\partial(\sigma_{ob_n}^0 - \sigma_{mod_n}^0)^2}{\partial x_n} \end{bmatrix}$$

Therefore, the computed model parameters of MWCM were found as A = 0.058, E =1.732, B = 0.201, C = -16.32, D = 23.76 using above computational techniques.

6.3.2.2. LUT generation with forward MWCM modeling

In the forward modeling steps, the in-situ measurements (calibration) of biophysical parameters and soil parameters were used to compute the model backscattering coefficient using developed MWCM and forward modeling algorithm. The computed model parameters (A, E, B, C and D) during the model calibration were used for the forward modeling. At each calibration step, the geocoded backscatter coefficient (VV, and VH) were simulated from the calibrated MWCM for each region 1 and 2 and subsequently the look-up table was generated. Furthermore, these LUTs were then used to feed the MTRFR.

6.3.2.3. Multi-target Random Forest Regression (MTRFR)

Segal (1992) demonstrated a multivariate regression trees which are based on the least squares optimization split function. In univariate response regression tree, the main role for least square optimization functions is to minimize the sum of squared errors (SSE) in the child nodes. Therefore, its target is to make partition of tree responses into two child nodes i.e. left node t_L and right node t_R. Thus, the task was to minimize the split function (θ) as,

$$\theta(s,t) = SSE\ (t) - SSS\ (t_R) - SEE(t_L) \tag{6.8}$$

Where, SSE (t) can be defined in term of $\bar{\varphi}$ (mean of each child node) and ith node φ_i as:

$$SSE(t) = \sum_{i=1}^{n}(\varphi_i - \bar{\varphi})^2 \tag{6.9}$$

Segal and Xiao (2011) demonstrated the multivariate random forest ensemble techniques added by covariance weighted function developed by Segal (1992). The significant prediction results were improved as compared to other computational techniques for multivariate as well as univariate predictions (Borchani et al. 2015). This can be expressed as:

$$SSE(t) = \sum_{i=1}^{n}(\varphi_i - \bar{\varphi}\,)'\ W^{-1}(t,\omega)(\varphi_i - \bar{\varphi}\,) \tag{6.10}$$

where W is a covariance weight and ω represents parameters which characterize the covariance structure.

6.3.3. Model performance indicators

The performance of the modified model for the retrieval of SM was also evaluated by analyzing the different indices such as percentage bias, RMSE and NSE.

6.3.3.1. Bias

The percentage bias has the average tendency of the retrieved values to be smaller or larger than their observed values. The optimum value of percentage bias is zero whereas; positive and negative values indicate the over and under estimated values by the model,

respectively. The percentage bias calculation can be made by the mathematical relation given as:

$$\text{Bias} = \frac{\sum_{i=1}^{n} \text{SM}_{\text{est}} - \text{SM}_{\text{ob}}}{\sum_{i=1}^{n} \text{SM}_{ob}} \tag{6.11}$$

Where SM_{ob} and $\text{SM}_{\text{est}}$are the observed and the estimated values by the models, respectively.

6.3.3.2. Nash Sutcliffe efficiency (NSE)

The NSE, a measure of the performance of the model, is computed as:

$$\text{NSE} = 1.0 - \frac{\sum_{i=1}^{n}(\text{SM}_{\text{ob}} - \text{SM}_{\text{est}})^2}{\sum_{i=1}^{n}\left(\text{SM}_{\text{ob}} - \widehat{\text{SM}_{\text{ob}}}\right)^2} \tag{6.12}$$

Where SM_{ob} andSM_{est} are the observed and the estimated values from the models, respectively while $\widehat{\text{SM}_{\text{ob}}}$ represents average value of the observed SM.

6.3.3.3. Root mean square error (RMSE)

The RMSE, a measure of the weighted variation in residuals between the observed and modelled values, is defined as:

$$\text{RMSE} = \sqrt{\frac{\sum_{i=1}^{n}(\text{SM}_{\text{ob}} - \text{SM}_{\text{est}})^2}{\text{N}}} \tag{6.13}$$

Where SM_{ob} and $\text{SM}_{\text{est}}$are the observed and the estimated values by the models, respectively and N is the total number of samples data.

6.4. RESULTS AND DISCUSSION

6.4.1. Correlation analysis between spatio-temporal retrieved soil moisture (SM) with backscattering coefficient (σ^0) derived from Sentinel-1A SAR data

The present study was focused on the estimation of SM by the developed MWCM of the fields covered with vegetation and sparse vegetation. The MWCM calibration and its parameters retrieval were performed to minimize the cost function using Equation 6.6 by the inclusion of training data sets like, SM, LAI and SAR derived σ^0 (dB). Moreover, the MTRFR inversion algorithm was adopted for the retrieval of soil moisture by Equations 6.2 - 6.4 to feed LUT techniques. Furthermore, the linear regression analysis was done between the retrieved soil moisture and backscattering coefficient to determine the potential of the inversion technique applied on the developed MWCM and improved inversion scheme. The computed σ^0 (dB) at VV polarization was found significantly correlated with the retrieved SM by the MWCM (R^2 = 0.78) as shown in Figure 6.5. Thus, the inversion result confirms that the inclusion of LAI and f_{veg} in the developed MWCM yielded high sensitivity of backscattering coefficient on the soil moisture retrieval which led to accurate retrieval of SM. This might be due to capability of the developed MWCM to separate the radar signal strength from the vegetation and soil surfaces due to incorporation of f_{veg} in the model.

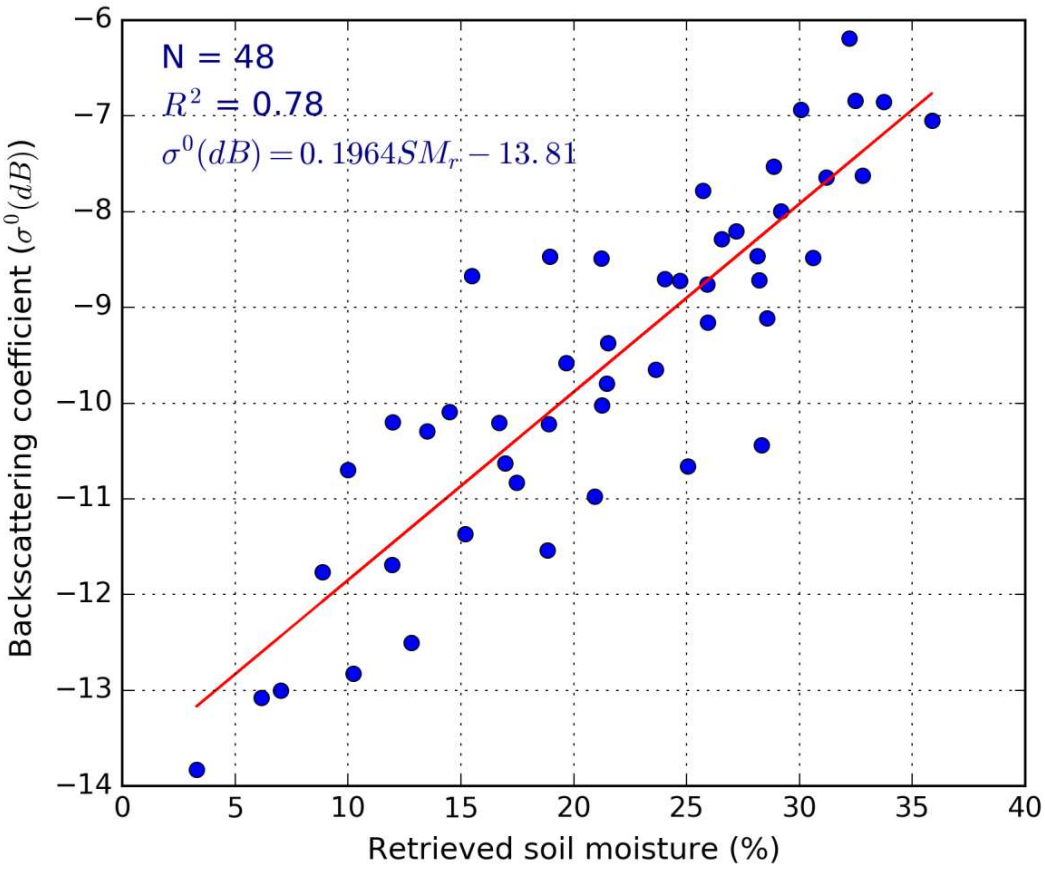

Figure 6.5 Linear regression between Sentinel-1A (SAR) observed backscattering coefficient and retrieved soil moisture through MWCM at VV polarization

6.4.2. Spatio-temporal mapping of soil moisture using MWCM

The flow chart for simulation of SM mapping is shown in Figure 6.4. In the pre-processing step, the input Sintenel - 1A images were calibrated, geocoded, and co-registered with Landsat-8 satellite data. The f_{veg} was computed from Lansat-8 images corresponding to geo-reference σ° (dB) values for the parameterization and calibration of MWCM. The MTRFR inversion algorithm was developed for the forward and inversion process of MWCM using training data (LAI, SM) and the geocoded σ° (dB) derived from Sentinel-1A SAR data for the retrieval of SM. Subsequently, the validation data sets were used for the inversion of

trained MWCM using MTRFR algorithm followed by LUT technique. Therefore, the final retrieved SM maps were generated pixel by pixel from the input σ° (dB) values. Land-use maps were considered for masking the areas like desert, rocks, urban areas, and water bodies where SM cannot be reliably measured. Figures 6.6 and 6.7 show the retrieved geo-referenced SM in the spatial region-1 and region-2, respectively. The temporal variations of retrieved SM in the regions 1 and 2 were found to be in the range of 4% to 26% and 5% to 37 %, respectively. Moreover, the soil fields mostly covered with wheat, barley, linseed, lentil, pea and other Rabi season crops were at growing, booting and heading stages during the measurements of SM and hence the change in soil moisture content during these growth periods was observed at the level of farmer's practices and irrigation methods. The spatio–temporal dependencies of f_{veg} on NDVI with different crop growth rates and hydrological conditions may have affected the retrieval of SM through MWCM at regional scales.

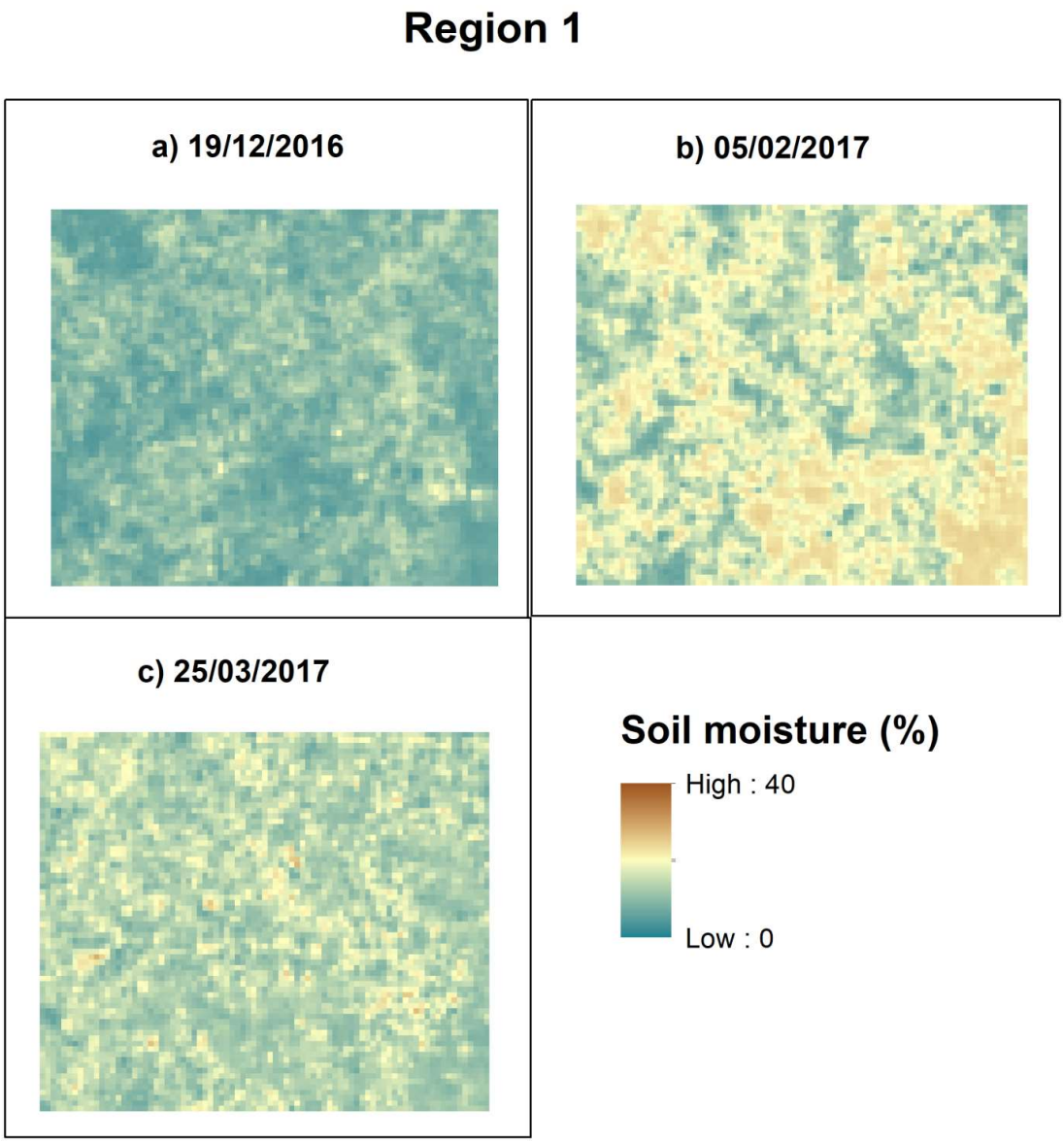

Figure 6.6. Temporal SM mapping for region 1 (sparse vegetated soil fields)

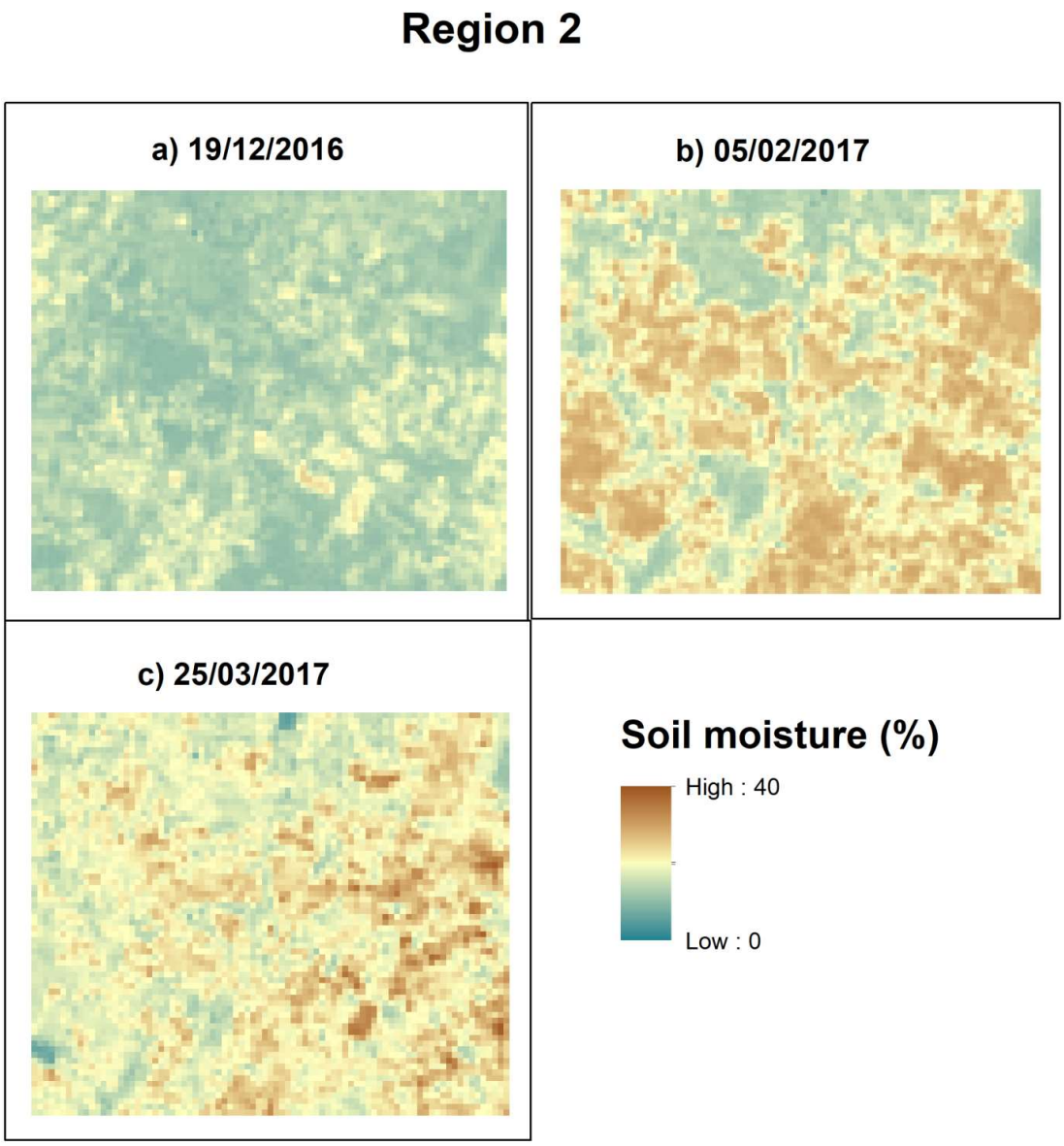

Figure 6.7. Temporal SM mapping for region 2 (vegetated soil fields)

6.4.3. Consistency of spatio-temporal SM retrieved through MWCM and in-situ measurements.

The present study shows that the developed MWCM has a great potential for accurate retrieval of SM covered with sparse and vegetated fields. The independent SM data sets not used in the model parameterization were taken for the validation of the model. Figures 6.8 and 6.9 show the values of retrieved SM by the developed MWCM and in-situ measurements

for the regions-1 and 2, respectively. Figure 8 shows that the consistency between the SM retrieved by MWCM and in-situ measurement in region-1 at three temporal changes of SM covered with sparse vegetated soil field. In the case of sparse vegetated soil field, the retrieval accuracy of SM was found quite low at VV polarization. However, the performance indices for the SM retrieval in the region-1 on 25/03/ 2017 date showed good statistical results (R^2 = 0.766, RMSE = 4.23% and NSE = 0.74) as compared to other two dates of SM retrieval. The details of retrieval of SM performance indices for the region-1 are shown in Table 6.3.

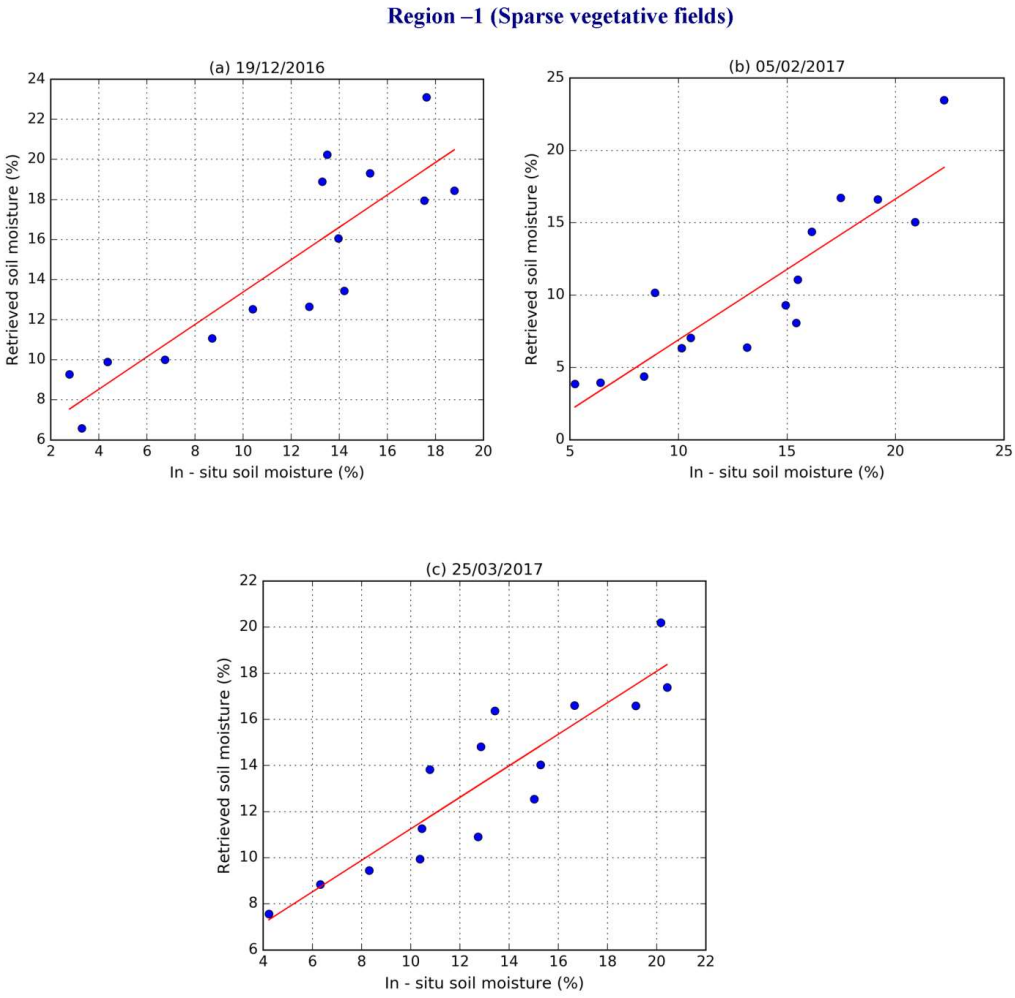

Figure 6.8. Temporal analysis between retrieved SM through MWCM and in-situ SM in region 1

Table 6. 3 Performance indices for retrieval of SM using MWCM in region 1

Soil field	Date	Linear fit equation (Y = retrieved *SM*, X = in-situ *SM*)	R^2	RMSE (%)	NSE	Bias
Region -1	19/12/2016	Y = 0.894X + 4.49	0.741	4.41	0.68	0.311
	05/02/2017	Y = 0.713X + 0.98	0.750	4.30	0.72	0.035
	25/03/2017	Y = 0.665X + 4.93	0.766	4.23	0.74	- 0.123

In the region-2, soil fields were covered mostly by wheat and barley crops. Figure 6.9 shows that the values of the retrieved SM by the developed MWCM were very close to the in-situ measured SM. The retrieval accuracy was found better in region-2 in term of high coefficient of determination (R^2) = 0.857, low RMSE = 3.15% and high NSE = 0.87 as compared to region-1 for the same date. The NSE parameter indicates the performance of MWCM model for the retrieval of SM in both the regions. The NSE indicated higher values (0.79 to 0.87) for all the temporal variation of SM in region-2 as compared to region-1 (0.68 to 0.74). Therefore, the statistical analysis shows that the MWCM has high potential for the accurate retrieval of SM in the vegetated area as compared to other soil field conditions at VV polarization. The detail specification of MWCM performance for the retrieval of SM in the region -2 is shown in the Table 6.4.

In the region-1, soil fields were mostly covered by sparse vegetation like lentil, linseed, pea and other less dense vegetated crop. Therefore, the radar signal is mostly attenuated by vegetation and soil interfaces which led to reduce soil contribution (σ^0 (dB))

over the region-1.Whereas, in region 2, the soil field covered with homogeneous canopy of wheat and barley crops led to coherent summation of radar signal. Figures 6.10 and 6.11 show the relative values of R^2 and RMSE for both the regions, respectively. The result indicated that MWCM has a good potential to discriminate the backscattering response from the vegetation and soil, which led to enhance the retrieval efficiency of SM in the region 2 as compared to region 1.

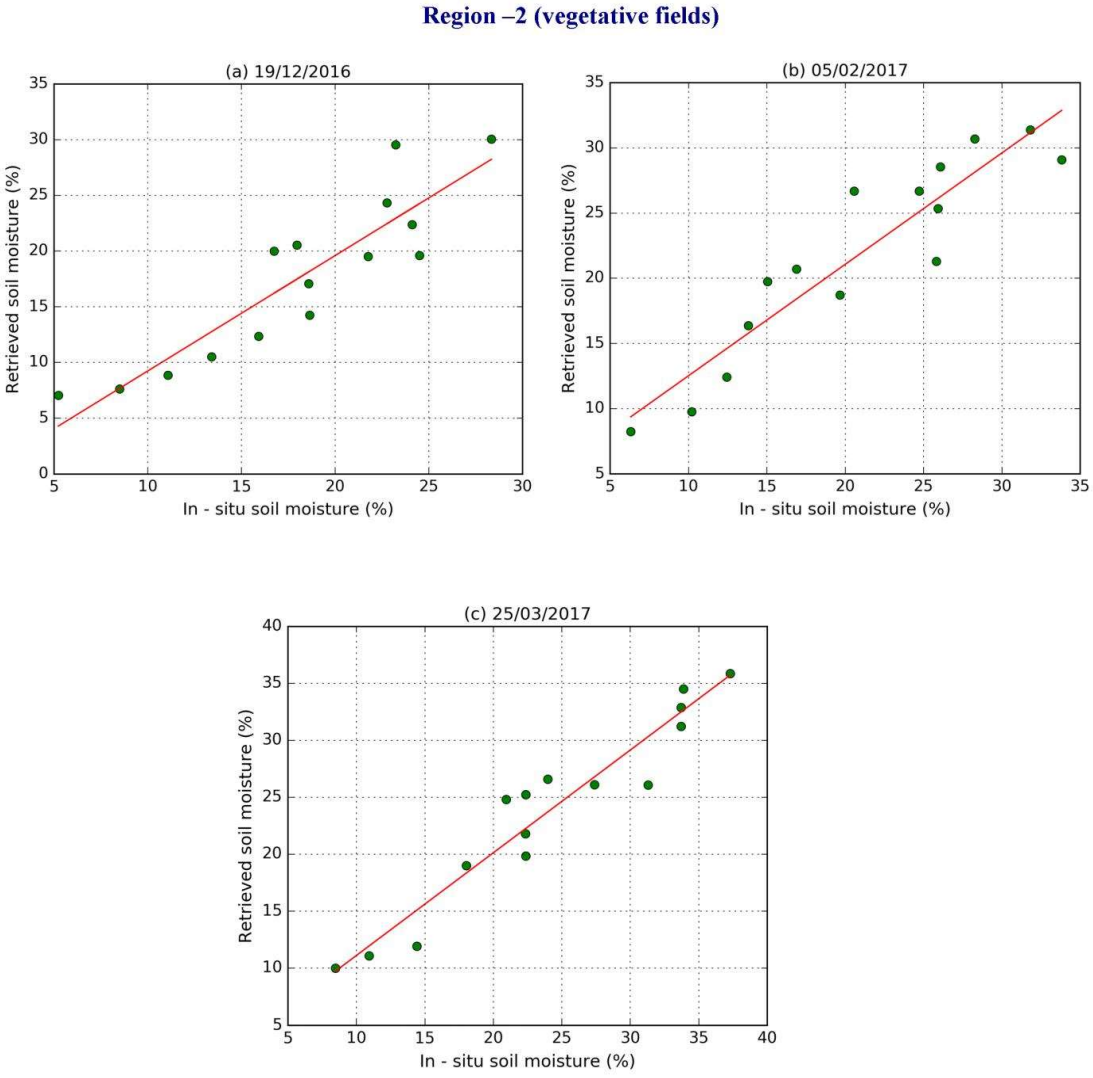

Figure 6.9. Temporal analysis between retrieved SM through MWCM and in-situ SM in region 2

Table 6.4 Performance indices for retrieval of SM using MWCM at region 2

Soil field	Date	Linear fit equation (Y = retrieved SM, X = in-situ SM)	R^2	RMSE (%)	NSE	Bias
Region - 2	19/12/2016	Y = 0.952X + 0.0562	0.791	3.38	0.79	-0.045
	05/02/2017	Y = 0.778X + 4.573	0.812	3.21	0.83	-0.015
	25/03/2017	Y = 0.918X + 0.133	0.857	3.15	0.87	-0.011

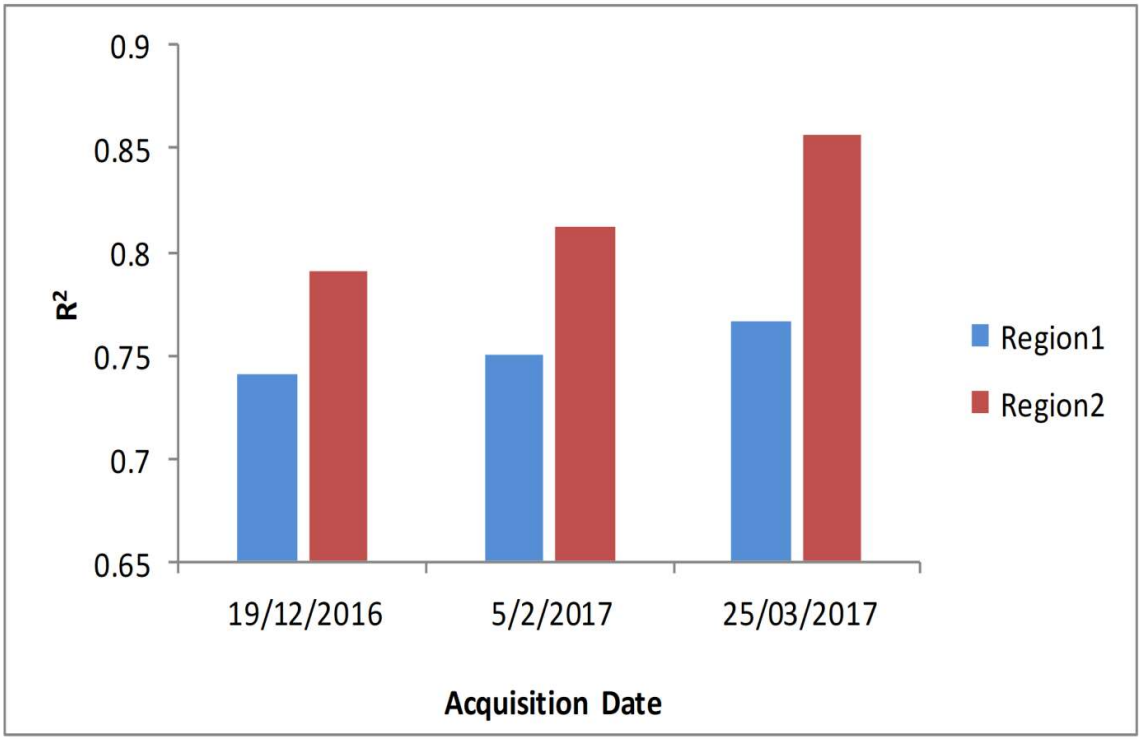

Figure 6.10 Temporal comparison of coefficient of determination (R^2) in region 1 and region 2.

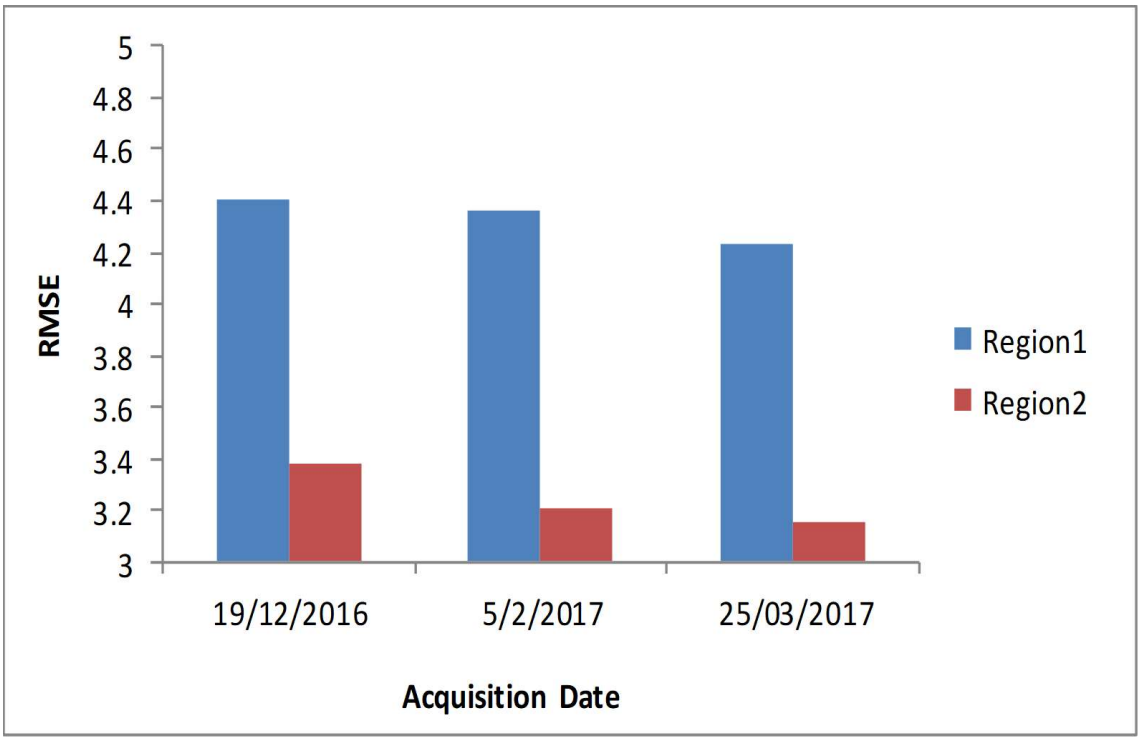

Figure 6.11 Comparative analysis of RMSE values in region 1 and 2 for robustness of the MWCM performance

The potential of MWCM for the spatio-temporal retrieval of SM was evaluated by computing NSE values. Figure 12 shows the efficiency of the MWCM for the retrieval of SM in the regions under investigation. NSE values showed higher performance in the region 2, where soil field was mostly covered by dense vegetation like wheat and barley. The region 1 showed lower NSE values as compared to region 2.

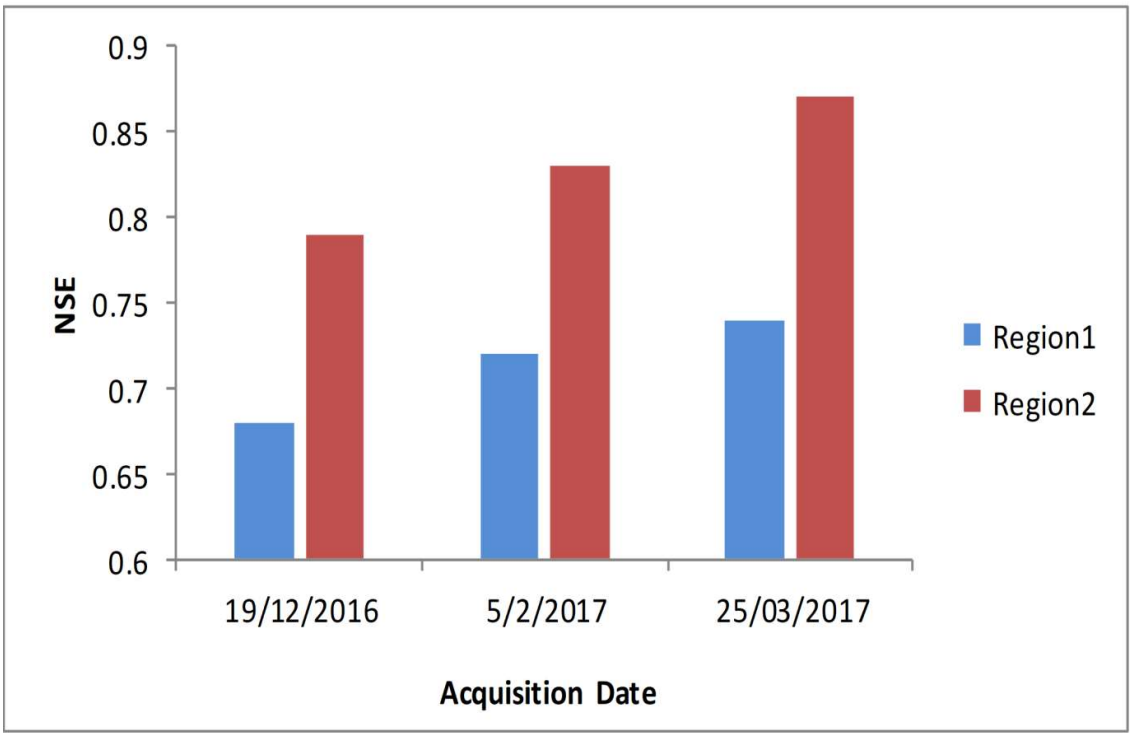

Figure 6.12 Comparative analysis of NSE values in regions 1 and 2 for evaluation of the MWCM performance

The developed semi-empirical MWCM provided better capability for the SM retrieval in the vegetated crop fields having LAI between 3 to 6 m^2/m^2. Figure 13 shows the overall accuracy of SM retrieval using (a) MWCM and (b) WCM. The result shows a good linear relationship between the retrieved SM by MWCM and in-situ SM measurements which is indicated by getting high R^2 = 0.82 and low RMSE = 3.18(%) as compared to the former WCM (R^2 = 0.73 and NSE = 0.72). Therefore, the results of the present approach indicate a good capability of the developed MWCM for accurate retrieval of SM covered by vegetated crop fields than that of old WCM.

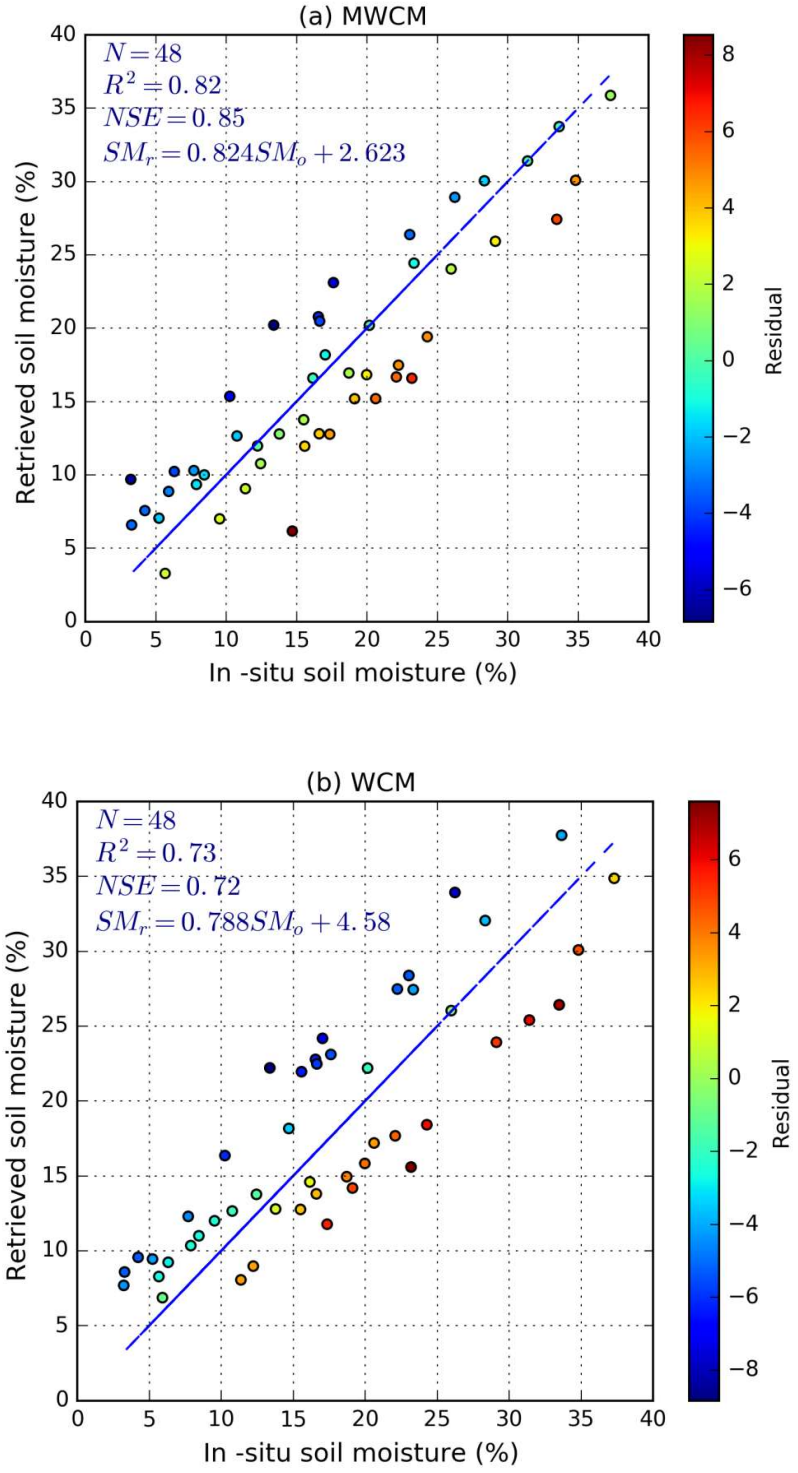

Figure 6.13. The overall comparison between retrieved SM and in-situ SM through (a) MWCM (b)WCM in region 1 and region 2

6.5. CONCLUSION

In the present study, the spatio-temporal SM was retrieved for Varanasi district, India, using Sentinel-1A satellite data at VV polarization with adoption of improved inversion algorithm. The semi-empirical MWCM backscattering model was developed by incorporating f_{veg} and LAI as vegetation parameters for the retrieval of SM. The f_{veg} were computed using Landsat-8 satellite data in the vegetated and sparse vegetated soil sample fields. The MWCM model parameters were computed using non-linear least square optimization technique by minimizing the cost function. After parameterizations of the MWCM, the MTRFR inversion algorithm was used for the retrieval of SM in the study regions -1 and -2 during all the temporal changes followed by LUT techniques. The values of R^2 and RMSE were found better in region - 2 covered mostly with wheat and barley crops. The present study revealed the following majors scientific out-comes:

1) The microwaves data acquired by Sentinel - 1A (central frequency 5.405 GHz) could be more robust for the monitoring of SM in vegetated and non-vegetated covered soil field due to capability of day-night data acquisition, higher penetration depth and independence of almost all weather conditions.

2) The f_{veg} factor, derived from well-known spectral reflectances based on normalized difference vegetation index (NDVI), played an important proportional parameter in MWCM to decoupled the synthetic aperture radar (SAR) signal strength backscattered from vegetation and soil surface. Therefore, it enhanced the MWCM capability to rectify the ill-posed retrieval problems where the vegetation and soil having the nearly equal reflectances.

3) In the present study, the MTRFR algorithm was selected for the regularization and inversion of MWCM followed by LUT. The MTRFR algorithm has capability to reduce the outlier noise and required minimum hyper-parameters as compared to others inversion

algorithms like iterative optimization (IO), ANN and SVM. Therefore, the MTRFR based inversion algorithm developed in present study provided the better inversion results as compared to inversion techniques applied in recent past to MWCM for the estimation of SM.

The results of the present study confirm the high potential of the developed semi-empirical MWCM and improved inversion algorithm to retrieve and mapping the spatio-temporal patterns of soil moisture using time - series Sentinel - 1A SAR data, which may become more time continuous with the constellation of Sentinel - 1A and Sentinel - 1B satellites in near future.